SLAC–PUB–5311
April 2, 1991
T/E

Measurement of the Inclusive Decay Properties of Charmed Mesons†

The MARK III Collaboration

D. Coffman, F. DeJongh, G. P. Dubois, G. Eigen, D. G. Hitlin,
C. G. Matthews, A. Mincer, J. D. Richman, W.J. Wisniewski, and Y. Zhu
California Institute of Technology, Pasadena, CA 91125

Z. Bai, M. Burchell, D. E. Dorfan, J. D. Drinkard, C. Gatto, C. A. Heusch,
W. S. Lockman, R. Partridge, H. F. W. Sadrozinski, M. Scarlatella,
T. L. Schalk, A. Seiden, A. J. Weinstein, S. Weseler, and R. Xu
University of California at Santa Cruz, Santa Cruz, CA 95064

J. S. Brown, B. I. Eisenstein, T. Freese, G. Gladding, J. M. Izen,
C. Simopoulos, I. E. Stockdale, B. Tripsas
University of Illinois at Urbana-Champaign, Urbana, IL 61801

U. Mallik and M. Z. Wang
University of Iowa, Iowa City, IA 52242

T. Bolton, T. E. Browder, K. O. Bunnell, R. E. Cassell,
D. H. Coward, S. Dado, C. Grab, P. C. Kim, J. Labs, A. Odian, D. Pitman,
R. H. Schindler, W. Toki, F. Villa, S. Wasserbaech, and D. Wisinski
Stanford Linear Accelerator Center, Stanford University, Stanford, CA 94309

T. H. Burnett, V. Cook, A. D. Li, R. Mir, P. M. Mockett,
B. Nemati, L. Parrish, and H. J. Willutzki
University of Washington, Seattle, WA 98195

Abstract

We report a high statistics study of the inclusive decay properties of the charmed D^0 and D^+ mesons, and the first inclusive study of the charmed D_s^+. The data are collected at $\sqrt{s} = 3.77\,\text{GeV}$ and $\sqrt{s} = 4.14\,\text{GeV}$ with the Mark III detector at the e^+e^- storage ring SPEAR. For each charmed meson species, the charged-particle multiplicity, the strangeness content of the final state, and the average π^0 multiplicity are determined.

Submitted to *Physics Letters*

† This work was supported in part by the U. S. Department of Energy, under contracts DE-AC03-76SF00515, DE-AC02-76ER01195, DE-AC02-87ER40318, DE-AC03-81ER40050, DE-AM03-76SF0034, and by the National Science Foundation.

Inclusive measurements of charmed meson decays may be employed to isolate the general characteristics of channels not otherwise detected through exclusive measurements. Comparisons between the charmed mesons D^0, D^+, and D_s^+ provide valuable information about the relative strengths of possible decay mechanisms, which themselves may favor specific final state mesons.#1 We have previously reported the inclusive semileptonic branching fractions of charmed mesons.[1] We present herein high-statistics measurements of the charged ($\pi^{\pm}$, $\mathrm{K}^{\pm}$) and neutral (π^0, K^0) multiplicities for D^0 and D^+ decays, and the first such measurements for the D_s^+. With the D_s^+ measurements, we estimate the fraction of D_s^+ decays that result in final states containing no visible strange particle pairs.

The analysis is based on a set of D *tagged* samples using kinematically isolated $D^0\bar{D}^0$ and D^+D^- events from $9.35 \pm 0.47\,\mathrm{pb}^{-1}$ collected at the $\psi(3770)$ and $D_s^+D_s^-\gamma$ events from $6.30 \pm 0.46\,\mathrm{pb}^{-1}$ collected at $\sqrt{s} = 4.14$ GeV with the Mark III detector.[2] A tagged sample is defined as the set of events where at least one of the D mesons of a produced pair (the tag) is fully reconstructed. To reduce systematic uncertainties in this analysis, we use only tags comprised of all charged particles. The D^0 tag decay modes are $D^0 \to K^-\pi^+$, $D^0 \to K^-\pi^+\pi^+\pi^-$, and $D^0 \to \bar{K}^0\pi^+\pi^-$. The third mode is not used in the determination of the inclusive kaon branching ratios since a D^0 tag cannot be distinguished from a $\bar{D}^0$. The D^+ tag decay modes are $D^+ \to K^-\pi^+\pi^+$, $D^+ \to \bar{K}^0\pi^+$, and $D^+ \to \bar{K}^0\pi^+\pi^+\pi^-$, and the D_s^+ tag decay modes are $D_s^+ \to \phi\pi^+$, $D_s^+ \to \bar{K}^0K^+$, and $D_s^+ \to \bar{K}^{*0}K^+$. Since the $\psi(3770)$ decays to a $D\bar{D}$ pair, for the D^0 and the D^+ tags the recoiling tracks come from a $\bar{D}^0$ or D^- decay, respectively. In the case of the D_s^+ tags, the recoiling particles are a γ and

#1 Hereafter, reference to a "D" implies reference to the D_s^+ as well as the D^0 and the D^+. Moreover, unless otherwise noted, reference to a state also implies reference to its charge conjugate state.

a D_s^-. The beam-constrained mass distributions[#2] for the D^0 and D^+ tag samples are shown in Figs. 1(a) and 1(b), respectively, while Fig. 1(c) shows the invariant mass distribution for D_s^+ tags. Clear signals are evident for each meson. Events are retained, as indicated in Fig. 1, in the signal region and also at lower masses (the *sideband* region) for use in background evaluations. The number of entries above background in the signal region consists of 2780 ± 60 D^0, 1770 ± 50 D^+, and 66 ± 10 D_s^+ tags, where the errors reflect statistical uncertainties only.

The produced charged-particle multiplicity distribution p_j is obtained by unfolding the observed multiplicity distribution d_i with the use of an efficiency matrix ϵ_{ij} and subtracting the tag background distribution b_i using the sideband information:[3]

$$\sum_j \epsilon_{ij}\, p_j \;+\; b_i \;=\; d_i\,. \tag{1}$$

In the multiplicity count, a recoiling charged track must successfully pass a helix track fit in the drift chamber and satisfy $|\cos\theta| < 0.85$, where θ is the polar angle of the track with respect to the beam axis. Furthermore, the distance of closest approach between the track and the beam axis must be less than 40 mm.

The matrix ϵ_{ij} contains the efficiency for observing i tracks when j are produced. It is determined for D^0, for D^+, and for D_s^+ using Monte Carlo simulations of the tracking chamber response to their decays. In these simulations measured branching ratios and estimates of unmeasured branching ratios are utilized.[4] Since the efficiencies depend predominantly upon detector acceptance, the uncertainties introduced by an incomplete knowledge of these branching ratios will be reflected only in second

#2 The beam-constrained mass is defined as $M_{bc} \equiv \sqrt{E_{beam}^2 - (\sum_i \vec{p}_i^{\,2})}$ where E_{beam} is the electron beam energy and $\vec{p}_i$ is the momentum vector for the i^{th} tag daughter.

order in these results. This approach reproduces well both the observed multiplicity of charged particles and their momentum spectra. To minimize systematic errors, the track selection and unfolding procedure does not distinguish particle types. Charged tracks from K_S^0 and other meson decays are included. Typical values for the D^0 diagonal elements ϵ_{22}, ϵ_{44}, and ϵ_{66} are 0.52, 0.20, and 0.033, respectively.

The resulting unfolded topological branching ratios and the average multiplicity obtained for each D type are listed in Table I.[#3] The primary sources of systematic errors include uncertainties in the sideband subtraction and the Monte Carlo modeling of the track selection. For each multiplicity, the contributions from each of these sources are estimated separately and combined in quadrature. The systematic error due to the tag sideband subtraction ranges from 0.5% for the most populated multiplicity bin to 11% for the least populated bin, and the contribution from ϵ_{ij} varies from 1% to 11% over the same range. The resulting D^0 and D^+ multiplicities are consistent with previous measurements,[5-7] but have significantly smaller errors. The D_s^+ result represents the first complete multiplicity measurement for the decays of this meson.

The inclusive branching ratios to both charged and neutral kaons are determined by identifying $K^\pm$ and $K_S^0 \rightarrow \pi^+\pi^-$ in the recoil of the tags. The charm of the tag is utilized explicitly to subdivide the charged kaon sample into "same-sign" and "opposite-sign" categories, where the sign is compared to that expected for a kaon originating from the decay of the charm quark (*e.g.*, in $D^+ \rightarrow \bar{K}^0 K^+$, the K^+ is an opposite-sign kaon). The charged kaons are identified by the time-of-flight (TOF)

#3 The topological branching ratios B_j are related to the unfolded multiplicities p_j by the equation $B_j = \frac{p_j}{n_{tags}}$, where n_{tags} is the total number of tags of the given D type. The average charged track multiplicity is given by $\langle n_c \rangle = \sum_j \frac{j \cdot p_j}{n_{tags}}$.

system, which separates pions and kaons by more than 2σ over the kinematically allowed momentum range. The K^0 inclusive branching ratio measurement is obtained by searching for reconstructed K_S^0 vertices from $\pi^+\pi^-$ combinations. To improve efficiency, no TOF particle-identification requirements are imposed for the pions. For the K_S^0 candidates, the reconstructed vertex is required to be displaced by at least 3 mm from the interaction point. To further purify the sample, a χ^2 is formed which measures the alignment of the projections of the vertex displacement vector and the reconstructed $\pi^+\pi^-$ momentum vector in the plane perpendicular to the beam axis. All $\pi^+\pi^-$ combinations with probability $P(\chi^2)$ less than 0.1% are rejected. Figures 2(a) and 2(b) show the observed K_S^0 signal opposite D^0 and D^+ tags (combined) and the D_s^+ tags, respectively.

The net number of observed kaons is obtained in each case after background subtraction using the tag sideband information. For the charged kaon measurements, a correction is also made for the misidentification of pions as kaons. A special consideration must be made in the case of $D^0 \to K^-\pi^+$ tags, where the high momentum of the tag secondaries results in a 2% probability for the interchange of the π and K identifications, in turn switching the assignment of the "same" and "opposite" signs for the recoiling kaons. A 2% correction to the same-sign branching ratio and a 35% correction to the opposite-sign branching ratio is made.

The momentum-dependent efficiencies for same- and opposite-sign charged kaons and neutral kaons are determined using the Monte Carlo sample. Typical efficiencies are 45% and 27% for charged kaon and K_S^0 detection, respectively. Figure 3 shows comparisons of the observed charged and neutral kaon momentum spectra with the Monte Carlo model for each of the D^0, D^+, and the D_s^+. Good agreement is observed for the D^0 and the D^+. However, lack of knowledge about the D_s^+ branching ratios and limited statistics make a definitive comparison difficult.

Table II lists the final results for each D type. The results are consistent with previous measurements.[5,6] The systematic uncertainties for the charged kaon branching ratios include the model-dependence of the detection efficiency (2–9%), the uncertainties in tag sideband subtraction (2–13%), the total number of tags (6–13%), the TOF modeling (3%), and the tracking efficiency (1%). For the neutral kaon branching ratios TOF modeling does not contribute. The systematic errors are separately determined and combined in quadrature for each measurement.

The measurement of the average π^0 multiplicity $\langle n_{\pi^0} \rangle$ is extracted from all $\gamma\gamma$ combinations. The photon selection is complicated by the modest resolution of the shower counter $(18\%/\sqrt{E})$ and the existence of spurious showers which arise from albedo, interactions of hadrons in the shower counter, and electronic noise. To minimize these backgrounds, all photon candidates are required to be detected in at least two layers of the shower counter, to be separated by more than 18 degrees from the nearest charged track, and to have a measured energy of at least 60 MeV. Due to the photon selection requirements the π^0 detection efficiency depends significantly on its momentum.

For the D^0 and the D^+, a measurement of $\langle n_{\pi^0} \rangle$ is made separately for each 200-MeV-wide π^0 momentum bin to minimize the dependence of the detection efficiency on the momentum spectrum. Using the Monte Carlo simulation, an average detection efficiency ranging from 10% at 0.1 GeV/c to 64% at 0.9 GeV/c is obtained for each bin. Figure 4 shows the sideband-subtracted $\gamma\gamma$ mass spectrum for each momentum bin. The number of π^0's is determined by a fit to the sum of a π^0 line shape obtained from Monte Carlo simulation and a π^0 background shape obtained from event-mixing. In event-mixing, photons from each event are combined with those of a previously tagged event having both the same photon multiplicity and the same photon energy distribution. To model the kinematics as closely as possible, only photons of similar energy are interchanged. In the fits which appear in Fig. 4, only the normalizations of the signal and background shapes are varied. The dominant systematic uncertainty in the π^0 signal arises from the uncertainty in the background shape derived from event-mixing. To estimate this uncertainty, the event-mixing technique itself is varied, and additionally, the fitting procedure is tested against the Monte Carlo model wherein efficiencies are known *a priori.* We estimate a 6% uncertainty from event-mixing for π^0 momentum bins above 0.2 GeV/c, where detection efficiencies are high and the small background arises predominently from the combinatorics of real photons.[#4] Other contributions include the tag sideband subtraction (6–12%), the number of tags (6%), the π^0 detection efficiency (4%), and the photon detection modeling (4%). Table III summarizes the $\langle n_{\pi^0} \rangle$ results for the D^0 and the D^+.

For the D_s^+ the low tag statistics do not allow binning by momentum. Instead, an average detection efficiency (23%) is calculated using a model of D_s^+ decays which reproduces the average charged pion and kaon multiplicities observed in the data. Event mixing is again used to estimate the background. We find 30 ± 17 π^0's above background, yielding an average π^0 multiplicity of $\langle n_{\pi^0} \rangle_{D_S^+} = 2.0 \pm 1.1 \pm 0.8$. The sources of systematic error are the model-dependence of the π^0 detection efficiency (28%), the event-mixing technique (25%), the tag sideband subtraction (13%), the number of tags (13%), and the photon detection modeling (4%).

#4 An error of 100% is conservatively assigned to the signal for π^0 with momenta below 0.2 GeV/c. In this region, a large background subtraction (relative to the signal) arising from the presense of many low energy photons is required.

In summary, we have presented inclusive measurements of the D^0 and D^+ which are consistent with but statistically improved over all previous experiments.[5,6,7] In addition, the first measurements of inclusive D_s^+ decay properties have been presented.#5 Our measurements indicate several notable differences between the D^+ ($c\bar{d}$) and the D_s^+ ($c\bar{s}$). The first such difference is the larger fraction of opposite-sign kaons in the D_s^+ as compared to the D^+. A larger fraction of opposite-sign kaons is expected in the naive Spectator Model of charm decay where their origin is from Cabibbo-allowed processes in D_s^+ decays and Cabibbo-suppressed processes in D^+ decays. Two other distinctions are the somewhat larger mean charged multiplicity (evident from the five-prongs), and the smaller total strange particle content of the D_s^+. From our data we estimate the fraction of D_s^+ decays which do not contain a $K\bar{K}$ in the final state as $B(D_s^+ \to \text{non}(K\bar{K})X) = 0.64 \pm 0.17 \pm 0.03$.#6 This result suggests either a significant rate for final states containing η or η', or a large non-spectator contribution, or both.

We gratefully acknowledge the dedicated efforts of the SPEAR staff. This work was supported by the Department of Energy, under contracts DE-AC03-76SF00515, DE-AC02-76ER01195, DE-AC03-81ER40050, DE-AC02-87ER40318, DE-AM03-76SF00034 and by the National Science Foundation.

#5 The direct knowledge of the complete D_s^+ multiplicity distribution may be combined with the results of Reference 8 to allow a model-independent determination of $B(D_s^+ \to \phi\pi^+)$ (see Reference 3, page 66). The result obtained is $B(D_s^+ \to \phi\pi^+) = 6.3\ ^{+3.2}_{-2.9} \pm 1.0\%$.

#6 Ignoring Cabibbo-suppressed decays, this branching ratio is estimated by: $B(D_s^+ \to \text{non}(K\bar{K})X) = 1 - \frac{1}{2}[B(D_s^+ \to K^+X) + B(D_s^+ \to K^-X) + B(D_s^+ \to K^0(\text{or } \bar{K}^0)X)]$.

References

1. Mark III Collab., R. Baltrusaitis *et al.*, Phys. Rev. Lett. **54**, 1976 (1985); Mark III Collab., Z. Bai *et al.*, Phys. Rev. Lett. **65**, 686 (1990).
2. Mark III Collab., D. Bernstein *et al.*, Nucl. Instrum. Methods **226**, 301 (1984).
3. B. Nemati, Ph.D. Thesis, University of Washington (1990), unpublished.
4. Particle Data Group, G. Yost *et al.*, Phys. Lett. **B204**, 1 (1988).
5. Mark I Collab., V. Vuillemin *et al.*, Phys. Rev. Lett. **41**, 1149 (1978).
6. Mark II Collab., R. H. Schindler *et al.*, Phys. Rev. **D24**, 78 (1981).
7. LEBC-EHS Collab., M. Aguilar-Benitez *et al.*, Z. Phys. C **36**, 551 (1987).
8. ACCMOR Collab., S. Barlag *et al.*, Z. Phys. C **48**, 29 (1990).
9. Mark III Collab., J. Adler *et al.*, Phys. Rev. Lett. **63**, 1211 (1989); **63**, 2858(E) (1989).

TABLE I. Topological branching ratios in percentages and average charged track multiplicities for each D type.

	D^0	D^+	D_s^+
B_0	$5.4 \pm 0.9 \pm 0.6$		
B_1		$38.4 \pm 1.8 \pm 1.5$	$37 \pm 10 \pm 3$
B_2	$63.4 \pm 1.5 \pm 1.9$		
B_3		$54.1 \pm 2.2 \pm 0.5$	$42 \pm 15 \pm 3$
B_4	$29.3 \pm 1.8 \pm 1.5$		
B_5		$7.5 \pm 1.3 \pm 0.7$	$21 \pm 11 \pm 3$
B_6	$1.9 \pm 0.9 \pm 0.2$		
$\langle n_c \rangle$	$2.56 \pm 0.04 \pm 0.03$	$2.38 \pm 0.04 \pm 0.05$	$2.69 \pm 0.31 \pm 0.11$

TABLE II. D inclusive kaon branching ratios in percentages.

	D^0	D^+	D_s^+
$B(D \to K^- X)$	$60.9 \pm 3.2 \pm 5.2$	$27.1 \pm 2.3 \pm 2.4$	$13\ ^{+\ 14}_{-\ 12} \pm 2$
$B(D \to K^+ X)$	$2.8 \pm 0.9 \pm 0.4$	$5.5 \pm 1.3 \pm 0.9$	$20\ ^{+\ 18}_{-\ 13} \pm 4$
$B(D \to K^0(\text{or } \bar{K}^0)\ X)$	$45.5 \pm 5.0 \pm 3.2$	$61.2 \pm 6.5 \pm 4.3$	$39\ ^{+\ 28}_{-\ 27} \pm 4$

TABLE III. D^0 and D^+ $\langle n_{\pi^0} \rangle$ measurements for each π^0 momentum bin. For each D type, the total $\langle n_{\pi^0} \rangle$ is obtained by summing the results for all π^0 momentum bins.

p_{π^0} (GeV/c)	$\langle n_{\pi^0} \rangle^{D^0}$	$\langle n_{\pi^0} \rangle^{D^+}$
0.0–0.2	$0.19 \pm 0.14 \pm 0.19$	$0.23 \pm 0.18 \pm 0.23$
0.2–0.4	$0.73 \pm 0.09 \pm 0.09$	$0.56 \pm 0.10 \pm 0.08$
0.4–0.6	$0.24 \pm 0.03 \pm 0.03$	$0.24 \pm 0.04 \pm 0.04$
0.6–0.8	$0.11 \pm 0.01 \pm 0.02$	$0.13 \pm 0.02 \pm 0.02$
0.8–1.0	$0.040 \pm 0.004 \pm 0.006$	$0.018 \pm 0.004 \pm 0.003$
Total:	$1.31 \pm 0.17 \pm 0.21$	$1.18 \pm 0.21 \pm 0.25$

Figure Captions

1. Beam-constrained mass for the D^0 (a) and the D^+ (b) tag samples. For the D_s^+ tag sample (c), the invariant mass after kinematic fit[9] is used. The dark shaded regions denote the signal and the light shaded regions the sideband. In all three cases, the number of background events under the signal peak is determined by parameterizing the background shape as a polynomial with an error-function high-mass cutoff.

2. Observed $\pi^+\pi^-$ invariant mass spectrum showing the K_S^0 signal for (a) the combined D^0 and D^+ samples and (b) the D_s^+ sample.

3. The observed charged and neutral kaon momentum spectra for the D^0, D^+, and the D_s^+. The corresponding spectra in the Monte Carlo sample are shown in the solid histograms. The vertical scales are arbitrary.

4. The invariant $\gamma\gamma$ mass after sideband subtraction for consecutive momentum intervals of width 0.2 GeV/c. The D^0 results appear in frames (a) through (e), while the D^+ results appear in (f) through (j). In each frame, the dashed curve represents the background and the solid curve represents the sum of the signal and the background.

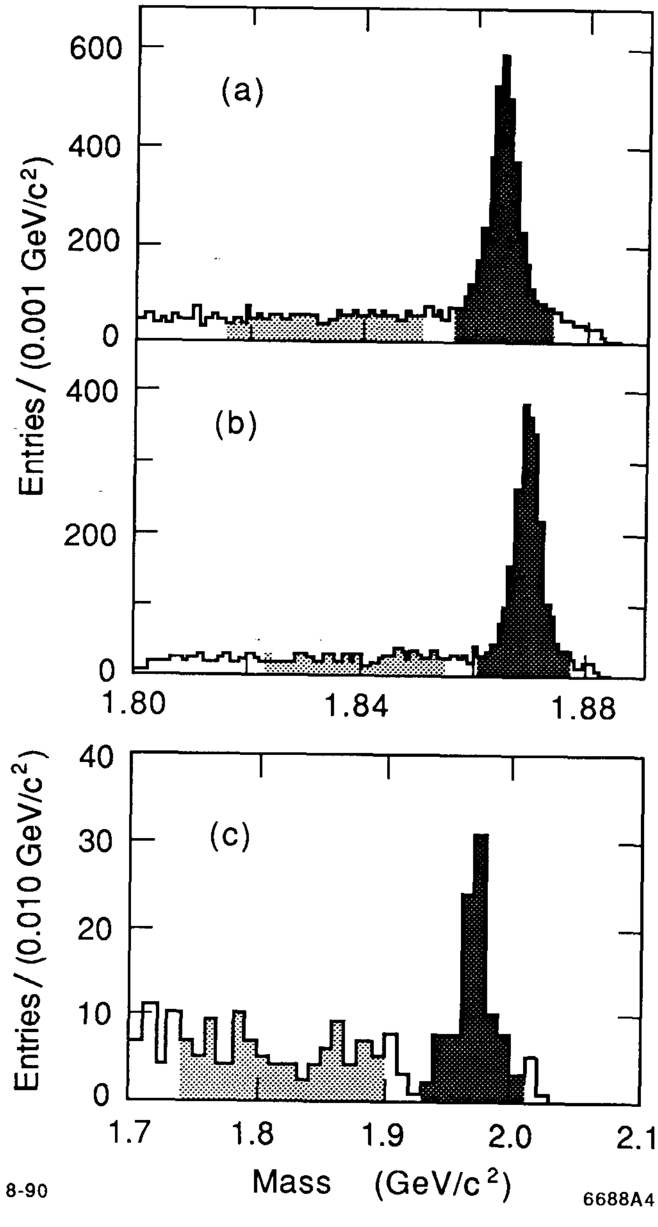

600
400
200
0
(a)
400
200
0
(b)
Entries / (0.001 GeV/c²)
1.80
1.84
1.88
40
30
20
10
0
(c)
Entries / (0.010 GeV/c²)
1.7
1.8
1.9
2.0
2.1
Mass (GeV/c²)
8-90
6688A4

Fig. 1

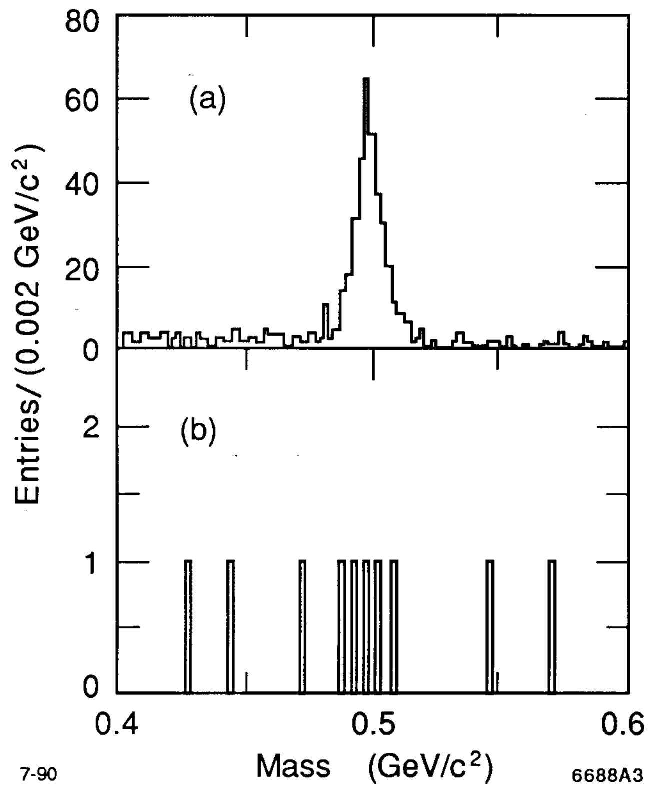
80
60
40
20
0
(a)
2
1
0
(b)
Entries/ (0.002 GeV/c²)
0.4
0.5
0.6
Mass (GeV/c²)
7-90
6688A3

Fig. 2

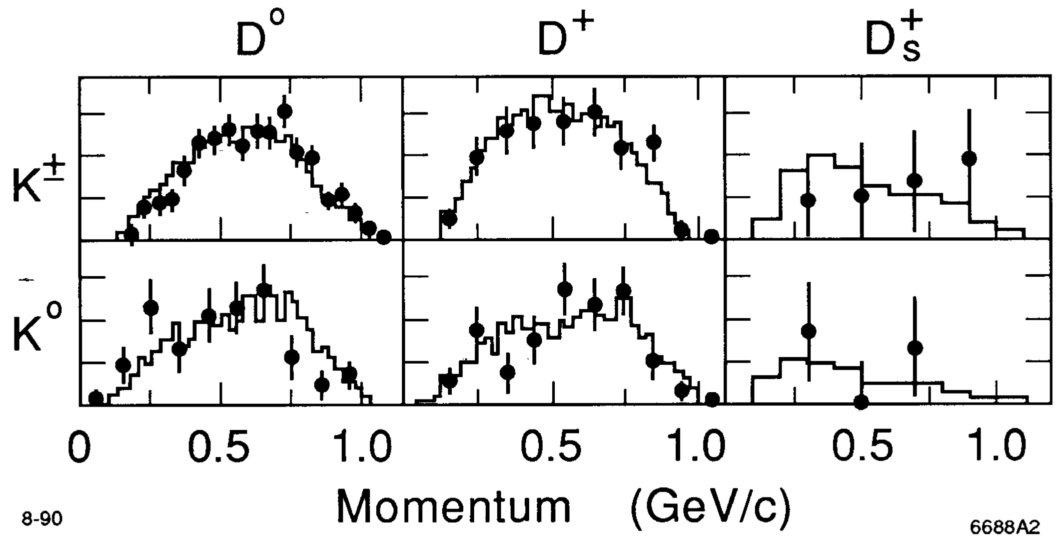

Fig. 3

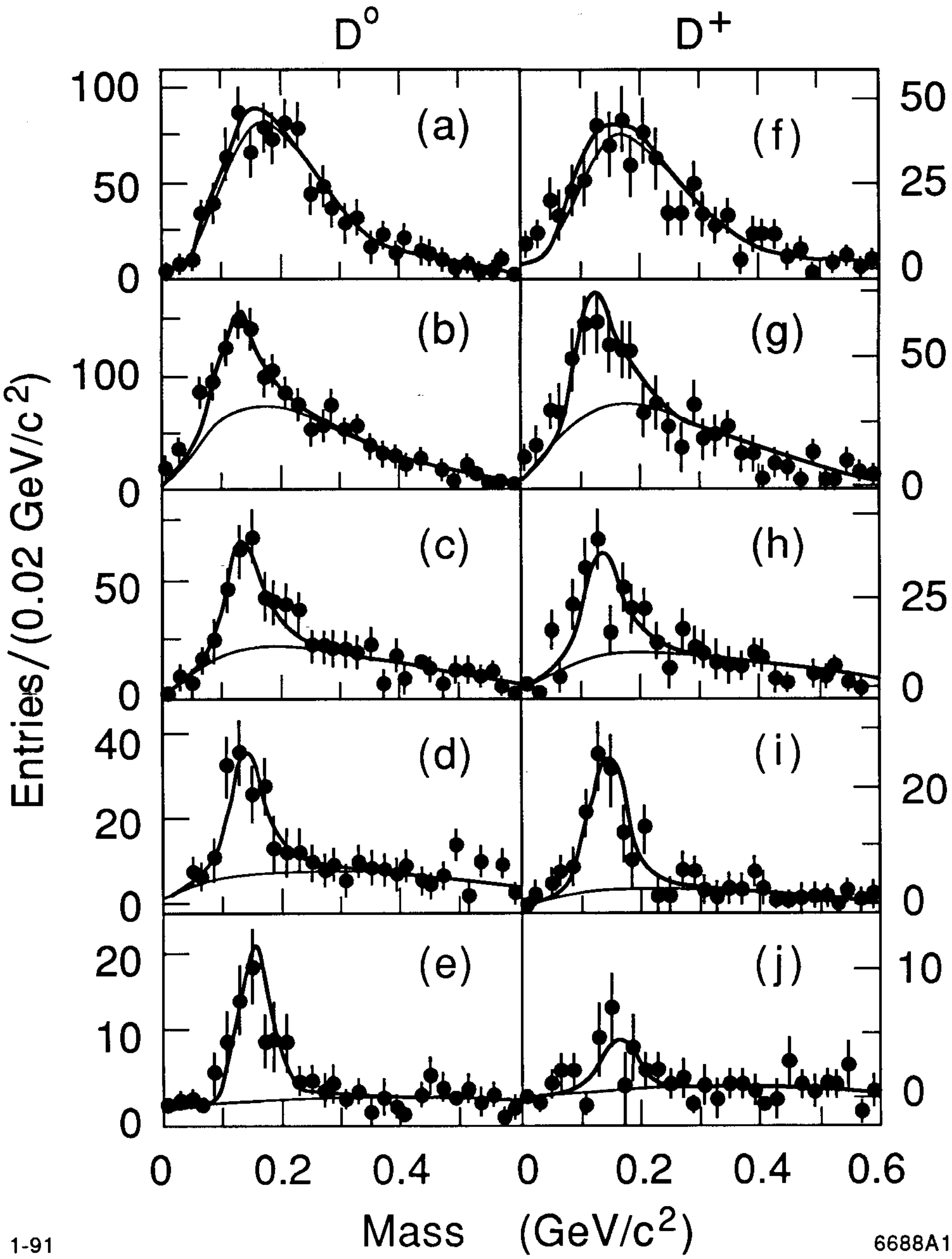

Fig. 4